

Title:

**Part VI: Quantum Mechanics and Physisorption - Mesoporosity**

**Author: James Condon\*†**

**Professor Emeritus**

\*Prof. Emeritus for the Regents College and Universities of the State of Tennessee, Roane State Community College, and former Senior Staff Member (Chemistry Research and Development) Oak Ridge Laboratories and adjunct full professor at University of Tennessee, and Gast Wissenschaftler Forschung Zentrum Juelich DE.

† Corresponding author. Email: [condonjb@genchem.net](mailto:condonjb@genchem.net)

© Copyright - October 2024 by James B Condon all rights reserved.

revised: 09.Jan, .2025

## Contents

<b>Abstract</b> .....	2
<b>Introduction</b> .....	3
<b>Calculating Mesoporosity: Volume, Area and Pore Size Distribution:</b> .....	3
Recognizing Mesoporosity .....	4
Fitting mesopore isotherms – the <b>D</b> function again and a new function $\chi^1$ .....	5
Example 1 – N <sub>2</sub> adsorbed on silicas (KIT-6):.....	6
<b>The Desorption branch calculated from the Adsorption branch.</b> .....	9
Example 2 The peak for mesoporosity GWMTK SBA-15 silica:.....	11
Speculation about calculating hysteresis:.....	<b>Error! Bookmark not defined.</b>
<b>Conclusion concerning mesoporosity:</b> .....	14
<b>What is next?</b> .....	14
<b>Appendix I about equations 1 and 2:</b> .....	<b>Error! Bookmark not defined.</b>
<b>References:</b> .....	15

Keywords: Physisorption, Quantum Mechanics, BET Theory, physical adsorption, micropores, mesopores

**Abstract:**

The determination of the parameters for mesoporosity requires knowledge from the previous parts for this series. The basic equations are that obtain with the creation of the  $\chi$ -plot and the  $\Delta\chi$ -plot and the log-law-plot. Compensation for the heterogeneity is needed to get the best resolution but may be bypassed by beginning above the value for  $n_a = 0$ . However, this might insert undesirable uncertainty in the calculation and, if the equipment is capable, data should be obtained at least into the HV and preferably in the UHV. Regardless of the initial appropriate plot, the mesoporosity is a modification using the cumulative normal distribution, **D**, or the inverse  $\chi$ -function,  $\chi^{-1}$ , for the simple case of one type of mesoporosity. If there is microporosity, the two might be separated enough from each other that an analysis is possible.

The mesoporosity is calculated by inserting function **D** or  $\chi^{-1}$  into the calculation. Both the adsorption and desorption may be analyzed this way. Often, hysteresis accompanies mesoporosity. It is too early in the development to claim this can be predicted. Suggestions are provided for a possible explanation. However, the only certainty is that the use of the **D** or  $\chi^{-1}$  function provides a very good fit to a simple case. If there are more than one size of mesoporosity with a broad distribution, a more sophisticated least square method might separate the sizes. The possible origins for hysteresis are presented with example calculations.

Main text:

## Introduction

So far in Parts I through V. the following has been addressed:

Part I The absolute disproof for various isotherm equations, including the BET, was presented. This provides reason for the search for new hypotheses of physisorption to be brought forth.

Part II A list of experimental problems and processes is provided. The definition of the thermodynamic system is clarified and the common experimental errors in the literature are listed. These errors are very common with the popular commercial instruments, so advice is provided as to how to overcome these errors with minor modification.

Part III This part goes into more detail about the BET and provides a possible way to use the two parameters of the BET to recalculate the quantum mechanical output parameters from them. It also demonstrate why the ordinate transform for the BET graphical analysis method is mathematically invalid. Furthermore, the standard deviations are incorrect regardless of how it arrived at. Use of a nonlinear least square eliminates the internal BET error, but the BET itself is wrong. Especially egregious is the determination of the standard deviation for the transformed BET plot – a terrible mathematical error. Never-the-less, a method is presented that correlates the BET answer with the QM. Of course, if one still has the original data, it can be recalculated using QM equations.

Part IV The resultant equations for QM hypothesis analysis are derived. This derivation is a general treatment and results in a universal equation used by others in the past as an empirical equation. However, the empirical equation has never been used to provide the proper energies and monolayer equivalence that are the point of the analysis. On the other hand, the QM seems to be quite universal for all numbered “Types” of isotherms except those that are obtain below the freezing point of the adsorbent. The QM It also provides a method of calculating the occupation of the admolecules densities in the various schichten (or “layers”) of adsorption. The hypothesis “Excess Surface Work” of ESW, a confirmatory hypothesis, is also introduced.

Part V The analysis of microporosity is provided with a special form of the QM schichten equations. This form is called the “log-law” as applied to a monolayer adsorption. Analysis of additional schichten is provided with some examples.

Part VI addresses mesoporosity including hysteresis

What is left to address in Part VII is calorimetric calculation and the relationship to the isotherm. The final section addresses binary adsorptive adsorption, which is very tentative since high quality data for testing is mostly missing.

### Calculating Mesoporosity: Volume, Area and Pore Size Distribution:

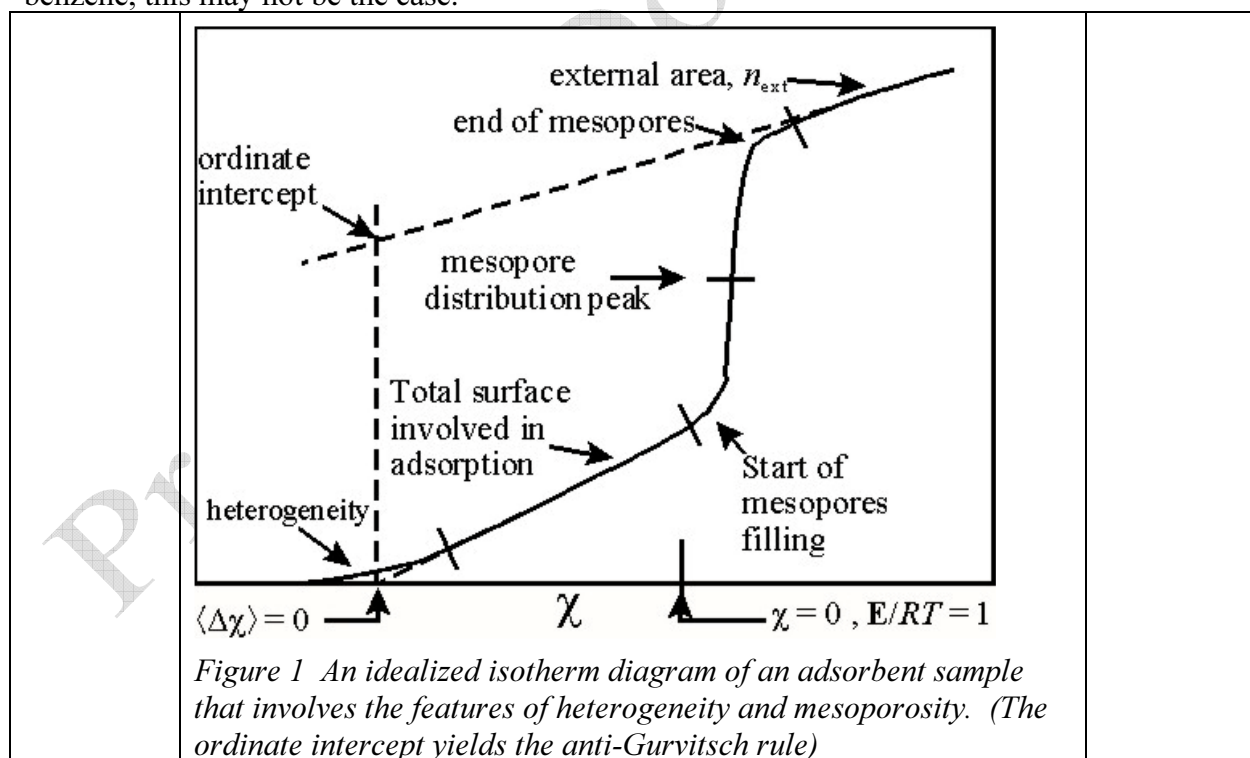
There is no question that the QM characterization is easy to do and easy to interpret compared to other techniques. However, the important question of prediction has not yet been addressed. It seems probable that a combination of QM and ESW will yield some answers.

In previous sections, the definitions of physical adsorption with the use of the QM formulation does not necessarily follow the SIO/IUPAC definitions. The IUPAC definitions of micropores and mesopores were classified according to the radius or pore wall separation. For the modern definitions, this is replaced by questions of what the interactions are between the adsorbent and adsorbate. This interaction is between  $E$  for the pore radii and the  $\Delta^{\text{a}}E$ . It is therefore based upon competing energies that determine the classification of micropore versus mesopore.

### Recognizing Mesoporosity

Mesoporosity is characterized by a positive curvature in the  $\chi$ -plot followed by a negative curvature\*. (A worthy note: An analysis that starts out linear in the  $\chi$ -plot can probably be analyzed using the classical method with the assumption that the  $n_m$  is obtained from the slope.) This usually results in a final linear portion for the  $\chi$ -plot, which has a slope less than the beginning slope. This is assuming that there are no other features that complicates the analysis. This feature begins normally at  $\chi \geq 0$  ( $-\Delta^{\text{a}}E/RT \leq 1$  or  $P/P_{\text{vap}} \geq 0.38$ .) This value of  $\chi$  is due to the energy considerations and not to the fact that it is the inflection point. A typical isotherm with these possible features are shown in *Figure 1* for multilayer isotherms.

For nitrogen the energy for at  $\chi = 0$  at 78 K is  $-648 \text{ J mol}^{-1}$ . One expects for the typical mesopore radii that the transition for mesoporosity onset is at a little higher value, perhaps about  $-300 \text{ J mol}^{-1}$  (Remember, think exothermic.) However, for other adsorptives, such as water or benzene, this may not be the case.



\* A worthy note: An analysis that starts out linear in the  $\chi$ -plot can probably be analyzed using the classical method with the assumption that the  $n_m$  is obtained from the slope.

If the pore filling calculates a value of  $\Delta\chi < 2$ , it might mean that hysteresis is not possible, since at least between 2 and 3 monolayer equivalence locally is needed to complete the gas liquid interface.

The hysteresis may be an artifact of a shifting  $E_a$ , but also not always. It seems to be the case that for some hysteresis loops they disappear when one plots  $\Delta\chi$  instead of  $\chi$ . This could make sense if the onset of pore filling is due only to competing energies since  $\chi$  is a measure of internal energy. The reason for the shift is unclear, but  $\Delta\chi$  is affected by any shift in  $P_c$ .

There has been much discussion about the origin of hysteresis in literature, but for this section only the question of where the mesoporosity begins is addressed. This section does not explain mesoporosity, neither why it starts for adsorption nor why there is hysteresis for desorption. Speculation will be presented after how to fit it experimentally to yield the relevant parameters. Once one has these parameters, than perhaps a reasonable mechanism can be demonstrated.

*Fitting mesopore isotherms – the  $\mathbf{D}$  function again and a new function  $\chi^1$ .*

The approach that is presented in this section is for fitting mesoporosity is as follows:

The first task is to characterize the mesopore phenomenon with a reliable equation. If the isotherm indicates two or several distinct isotherm onsets, then they are analyzed as separate isotherms as demonstrated in Part II. If not, then a distribution of  $E_{as}$  is the obvious conclusion.

However, the distribution of  $E_{as}$  is not relevant in a  $\chi$ -plot, only but only in a  $\Delta\chi$ -plot. The reason is that  $\chi$  value is the value of  $\Delta^a E$  for all the isotherms in the entire manifold. Thus, even though the individual isotherms within the distribution differ in starting  $E_{as}$ , they are added at the point at which they have identical  $\Delta^a E$ . This implies that if there is a distribution for the mesopore filling, it is due to a distribution of pore sizes or shapes randomly over a range. and not on the adsorbent heterogeneity. If nature is bias toward the normal distribution and if there are a variety of pore sizes and shapes, then the  $\mathbf{D}$  (Equation 9 Part II) function would apply to the mesopore feature. This additional feature is expressed in Equation 1.

$$\mathbf{n}_a = \mathbf{n}_{a,i} + (\mathbf{n}_{a,f} - \mathbf{n}_{a,i}) \mathbf{D}(x, \langle x_p \rangle, \sigma_p) \quad \text{Equation 1}$$

$$\text{where: } \mathbf{n}_{a,i} = (\Delta\chi n_m) \quad \text{and} \quad \mathbf{n}_{a,f} = (\Delta\chi n_{\text{ext}} + n_p)$$

Also, the following are the symbols used:

From here on the subscript “p” will be used to indicate either the  $\chi_p$ ,  $\Delta\chi_p$  or  $\mathbf{E}(\chi_p)$ , depending on choice, of the peak position of the distribution function for the pores. This subscript will also apply to the description of the distribution of the pores so:  $1\sigma_p$ .

$x$  can be either  $\Delta\chi$  or  $\chi$  depending upon preference.

$\mathbf{D}$  is the normal cumulative distribution,  $x_p$  = “peak” value,

$\langle x_p \rangle$  = ( $x_p$  for short) the peak of the pore distribution,  $\mathbf{G}$ , which is the differential of  $\mathbf{D}$ .

$\sigma_p$  = standard deviation (spread of  $\mathbf{G}$ )

$\mathbf{n}_{a,i}$  is the amounts amount of  $\mathbf{n}_a$  in the initial portion of the isotherm before mesopore filling is evident, and  $\mathbf{n}_{a,f}$  is the final amount after the filling. (This is assuming one type of pore. With several types one would have an initial and final portion for each type.)

The  $n_s$  are written as functions of either  $\Delta\chi$  or  $\chi$  and are, therefore, in bold font.

There is an alternative to *Equation 1*. This is the inverse  $\chi$ -function,  $\chi^{-1}$ .

$$\mathbf{n}_a(\chi) = [\mathbf{n}_{a,i}(\Delta\chi) - \mathbf{n}_{a,f}(\Delta\chi)]\chi^{-1} + \mathbf{n}_{a,f}(\Delta\chi) \quad \text{Equation 2}$$

where:

$$\chi^{-1} = \exp\{-\exp(\mathbf{arg})\} \quad \text{and} \quad \mathbf{arg} = \frac{\Delta\chi - \Delta\chi_p}{\sigma_p} \quad \text{Equation 3}$$

$\chi^{-1}$  function is related to the **D** function. Instead of squaring the inner argument, it is taken to the limit  $\infty$ . It is slightly skewed with a peak. For sharp peaks, low  $\sigma_p$ , this yields lower overall standard deviations,  $\sigma_{\text{fit}}$ , but for broad peaks the opposite seems to be the case. Many more experiments are needed to determine the usefulness of each function.

All this assumes that heterogeneity and mesoporosity do not overlap<sup>1</sup>. This seems unlikely because it appears that the mesoporosity is confined to be after the Fuller magic point,  $P/P_{\text{vap}} = 1/e$ , and heterogeneity is prominent before the magic point. Thus, if there is heterogeneity, then the values for  $n_a$  are calculated by the positive heterogeneity **Z** function, (See Part II - Heterogeneity). These values for  $n_a$  (now designated  $\mathbf{n}_a$ ,  $\mathbf{n}_{a,i}$ , and  $\mathbf{n}_{a,f}$ ) are modified by multiplying by the function for mesoporosity, in *Equation 1* or *Equation 2* and *Equation 3*.

If only one heterogeneity and one type of mesoporosity is present, then the final slope of  $\mathbf{n}_{a,f}$  in the equation yields the external monolayer equivalence. Furthermore, extrapolating  $\mathbf{n}_{a,f}$  back to  $\Delta\chi = 0$  yields the pore volume,  $n_p$  in term of moles, (the anti-Gurvitsch rule or the *ordinate* intercept for the extrapolated  $\mathbf{n}_{a,f}$  in the  $\Delta\chi$ -plot to yield  $n_{\text{ext}}^*$ .)

Obviously, these 3 new mesopore parameters, along with the 3 heterogeneous parameters<sup>†</sup> are best determined with a non-linear least squares routine. With heterogeneity and mesoporosity there are now 6 parameters. This includes the 3 parameters for  $\mathbf{n}_{a,i}$  of  $n_m$ ,  $\langle\chi_\zeta\rangle$  and  $\zeta$  and the 3 parameters for the switch to  $\mathbf{n}_{a,f}$  of  $\sigma_p$ ,  $\langle\chi_p\rangle$  (or  $\langle\Delta\chi_p\rangle$ ) and  $n_{\text{ext}}$ . In general, each feature adds 3 parameters.<sup>‡</sup>

Up to this point there is no supported hypothesis to specify the meaning of  $\langle\chi_p\rangle$  nor  $\sigma_p$  other than as fitting parameters. Obviously,  $\sigma_p$  is an indication of the distribution of pore cross-section areas, since the total pore volume is already determined by the anti-Gurvitsch rule. The position of  $\langle\chi_p\rangle$  is probably a trade-off in energies  $\Delta\Gamma^a\mathbf{E}(\chi)$  versus  $mA_p\gamma_{\text{lg}r}$  for a curved surface. This is addressed in the following section. This speculation will be presented after some examples of the fitting. Fitting the isotherm with a realistic analytical equation that has a low standard deviation helps in the interpretation.

*Example 1 – N<sub>2</sub> adsorbed on silicas (KIT-6):*

---

\* the ordinate for the log-law.

† Of course, if the plot does not approach  $n = 0$ , the heterogeneity cannot be measured and one has 2 parameters

‡ Recall that  $\zeta$  might be missing due to lack of low-pressure data and if a least square routine is used, it needs to be set of a very low number because 0 causes a computation error. If you then activate  $\zeta$  and it is negative that may mean you have detected the Knudsen effect.

This following is an example of a mesopore fit by Guillet-Nicolas, Marcous, and Kleitz<sup>2</sup>(GMK) and is KIT-6 (Prep details listed in the article.)<sup>\*</sup>. This was not measured below one monolayer equivalence. Unfortunately, absence of HV is typical, but some insight can still be obtained even though the  $\chi_c$  is uncertain. It apparently has one pore size. The adsorptive is N<sub>2</sub> at 78 K.

The data and the fit using  $\chi^{-1}$  are shown in *Figure 2*. The graph on the left is for the entire isotherm. The graph on the right is for the distribution of pores enlarged. The fits fulfill the requirement that the standard deviation be about 0.7 % of the full data range (FDR) for the desorption branch, but about 0.9 % FDR for the adsorption branch. Within the 1% FDR limit. The anti-Gurvitsch rule, which is the extrapolation to the ordinate of the  $\Delta\chi$ -plot, was used to obtain the pore volume.

The inverse chi function,  $\chi^{-1}$  is used for the pore distribution. In this case the **D** function yields only a slightly better fit to the data compared to  $\chi^{-1}$  as is indicated in Table 1 **Error! Reference source not found.**

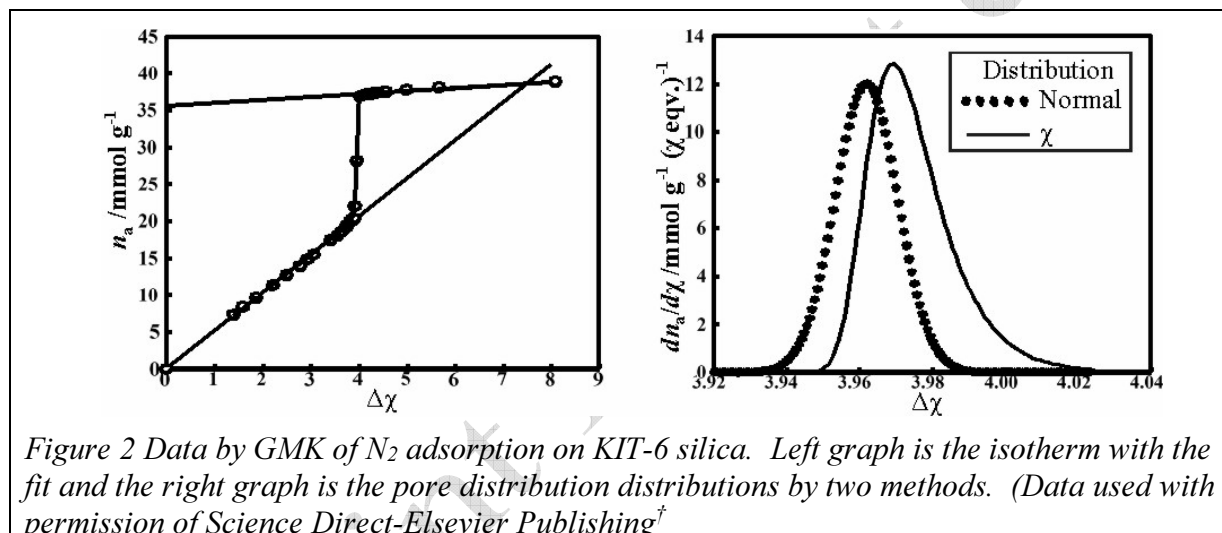


*Figure 2 Data by GMK of N<sub>2</sub> adsorption on KIT-6 silica. Left graph is the isotherm with the fit and the right graph is the pore distribution distributions by two methods. (Data used with permission of Science Direct-Elsevier Publishing<sup>†</sup>)*

In comparison of the data, there is not much difference between the normal distribution assumption and the  $\chi^{-1}$  assumption. A pressure correction was used but it is below the level of significance. In Table 1 are the output parameters of a non-linear least squares fit to this data. Some of the derived quantities will need further explanation presented in the next section.

<sup>\*</sup> Selection of examples depended upon the ability to read the graphs well enough to obtain enough datum points and if analyzed there appears to be no temperature problems.

<sup>†</sup> Since this peak is very sharp, one can detect a slight difference in the peak values between  $\chi^{-1}$  and **D**

<i>Table 1</i> parameters and quantities using the data by GMK of N <sub>2</sub> adsorption/desorption on KIT-6 silica that demonstrate the $\chi^{-1}$ versus <b>D</b> distribution and hysteresis value.				
physical quantity	Adsorption $\chi^{-1}$	Adsorption <b>D</b>	Desorption $\chi^{-1}$	Desorption <b>D</b>
$n_m$ /mmol g <sup>-1</sup> =	5.310	5.282	5.206	5.201
$\chi_s$ =	-2.9870	-3.0145	-3.0129	-3.0178
$n_{ext}$ mmol g <sup>-1</sup> =	0.661	0.679	0.680	0.715
$\Delta\chi_p$ =	4.259	4.275	3.997	3.995
$n_p$ /mmol g <sup>-1</sup> =	39.197	39.153	39.165	39.036
$\sigma_p$ =	0.0275	0.0304	0.0165	0.0227
Goodness of fits:				
$\sigma_{fit}$ /mmol g <sup>-1</sup> =	0.402	0.540	0.453	0.312
$\sigma_{fit}$ (FDR)/ % =	0.91	1.28	0.72	0.710
$r^2$ =	0.9990	0.998	0.9995	0.9995
Derived physical quantities:				
$\chi_p$ =	1.272	1.260	0.9682	0.9774
$n_{m,p}^\ddagger$ /mmol g <sup>-1</sup>	4.65	4.60	4.53	4.49
$E_a$ /kJ mol <sup>-1</sup> =	-12.69	-13.05	-13.02	-13.09
$E_p$ /J mol <sup>-1</sup> =	-181.7	-183.9	-242.2	-244.0
$A_p^\dagger$ /m=	454.3	449.4	442.6	438.3
$V_p(\rho_l)$ /mL g <sup>-1</sup> =	1.357	1.356	1.356	1.352
$r_p \leq 2V_p/A_p$ /nm =	5.97	6.03	6.13	6.17
$m\downarrow/m\uparrow$ * =	1.33	1.33		
* Ratio of desorption energy to adsorption energy, the $m$ s in the Equation 4				
† Conversion uses the IUPAC convention, $9.77 \times 10^4$ m <sup>2</sup> mol <sup>-1</sup> ‡ $n_{m,p} = n_m - n_{ext}$				

To obtain measurements that are not confined to moles but rather meters there needs to be some conversion factors used. All conversions used the IUPAC classical conversions. Furthermore, now, there is no settled way in QM to calculate the desorption branch of the hysteresis loop, despite the speculation below. Some possibilities seem logical:

- 1) The value for  $\chi_s$  shifts, perhaps from level of adsorbent surface contamination changing or



- 2) One might see a shift in the  $\Delta\chi$ -plot and not in the  $\chi$ -plot that eliminates hysteresis. This indicates that the mechanism is being controlled by the number of schichten adsorbed.
- 3) The geometry of the pore liquid-gas interface changed, for example from a 1D curvature to a 2D curvature affecting the parameter  $m$  in Equation 4 below<sup>3</sup>.

It may be that all these three phenomena and perhaps others are occurring. These other factors might be revealed with further research. This seems to be a fertile area of physisorption for research.

### The Desorption branch relationship to the Adsorption branch.

One of the discoveries that the QM model presented is the importance of the  $E_a$  and the Fuller point,  $\chi=0$  or  $P = 0.3678\dots$ , in the calculation of the desorption isotherm. Firstly, the  $E_a$  is the zero point for the  $n_a$ , whereas  $\chi = 0$ , is the reference point for the energy.  $\chi=0$  is also the inflection point for the isotherm. The at the “Fuller magic point” the QM model has an energy of  $-648.5 \text{ J mol}^{-1}$  for  $\text{N}_2$  at 78 K. The inflection point ( $\chi = 0$ ) is an important point in column operations (See Basmadjian<sup>4</sup>) since the second derivative in the isotherm plots changes from negative to positive at  $\chi = 0$ . This is always the case for any physisorption, barring some interference such as porosity. Furthermore, the slope of the untransformed, simple-case isotherm at this value is  $n_m$ . With this information one could speculate on the origins of hysteresis.

In some cases, hysteresis disappears or becomes much smaller in the  $\Delta\chi$ -plot. This means that the value of  $E_a$  has shifted. This may indicate that there is contamination or some other shift in the state of the starting (thermodynamic) system.

The shift to lower pressure for the desorption vis-à-vis adsorption is due to the shift from the QM with the schichten rules to classical surface tension mechanism, as described below.

In ESW the tensile strength of the liquid-gas interface determines the breaking and formation point for film formation.

The second and third possibility may be the same.

There are cases where hysteresis does not occur for more than monolayer adsorption is happening. In these cases, one makes the calculation by invoking the schichten equations and cannibalization, or alternatively, simply use the resulting  $\chi$ -plot to obtain the 6 (5 without heterogeneity) needed parameters. The reasons why hysteresis might not be observed include:

The pores are too small to accommodate more admolecules at the point that mesopore is calculated to happen.

$|E_a| < |\epsilon|$  which means the adsorbent is adsorbophobic.

There is another limitation for mesopore hysteresis, at least 2 schichten has to adsorb, at least locally. This implies that  $\Delta\chi \geq 2$ . At  $\Delta\chi = 2$  such a film is called a “black film” and usually very unstable, so perhaps the criterion is greater than 2, so that some internal liquid between the  $lg$  interface and the  $ls$  interface would be present.

Perhaps the important factor may be the difference between the energies of adsorption and desorption and the mechanism in one direction is different from another. This is illustrated in

Figure 3 The steps in the conversion between the QM dispersion (according to the schichten equations) and the compacted (classical theory) and the difference between adsorption and desorption., for cylindrical pores and using Equation 4 ( the Kelvin or Ostwald–Freundlich equation<sup>5</sup>.)

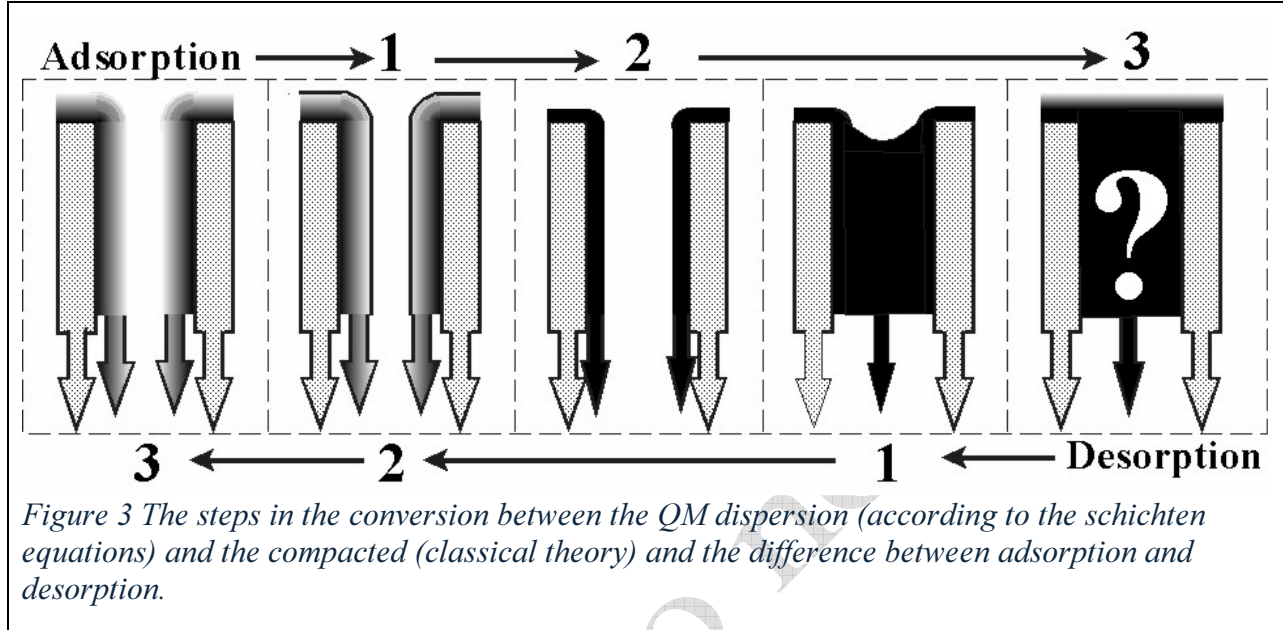


Figure 3 The steps in the conversion between the QM dispersion (according to the schichten equations) and the compacted (classical theory) and the difference between adsorption and desorption.

$$-RT \ln \left( \frac{P_p}{P_{\text{vap}}} \right) \cong \langle E_p \rangle := \Delta_l^a \mathbf{E}(\chi_p) = -\frac{m\bar{V}_l\gamma_{lg}}{r_c} \quad \text{or} \quad r_c = -\frac{m\bar{V}_l\gamma_{lg}}{\langle E_p \rangle} \quad \text{Equation 4}$$

Here and recalling  $E_s$  are negative, that is, exothermic and the approximate sign is for the very slight amount of entropy the missing in the Dubinin thermodynamic criterion.:

$m$  = geometric factor, which is  $m = 1$  for a film that has one uniform concave surface or  $m = 2$  for a film that has two equal concave surfaces, or something else for a variety of reasons. These values may have other value depending upon the specifics of the pore geometry.

$\gamma_{lg}$  = surface tension of adsorbate for the liquid-gas interface

$\bar{V}_g$  = molar volume of adsorptive liquid

$r_c$  = the classical “core” radius. The radius of an initial  $gl$  interface at the onset of mesoporosity.

The factor  $m$  can change, and in Figure 3 The steps in the conversion between the QM dispersion (according to the schichten equations) and the compacted (classical theory) and the difference between adsorption and desorption..is a simple model how this could be. This equation is normally called the Kelvin or Ostwald–Freundlich equation adapted for the tie to QM through  $\langle E_p \rangle$ , There have been many modifications made for physisorption and perhaps this is not the appropriate form. More research is needed to determine this

Referring to *Figure 3* The steps in the conversion between the QM dispersion (according to the schichten equations) and the compacted (classical theory) and the difference between adsorption and desorption. the mesoporosity in adsorption assumes uniform cylinders, where the pore filling is triggered by the adsorption reaching the energy of  $E_{p\uparrow}$ , which has a  $m_{\uparrow} = 1$ , that is, only the sides are covered by the diffuse QM layer (step 1,2 3 adsorption). For the desorption, the film, which does not “break” until a lower energy is reach and the semispherical surface is formed, (desorption steps 1,2 3) and  $m_{\downarrow} = 2$ . The question mark on the right most figure is about, “What is the external area?” As shown, it is assumed to include the covered pore entrance. Thus, a perfect cylindrical pore system, with no cross links and open pores that are perfectly matched to the pore walls will have a ratio of  $m_{\downarrow}/m_{\uparrow} = 2.00$ . This ideal system is probably rare so a distribution of pores and, thus, sizes and shapes are in order. This is asking a lot of just three parameters for the mesoporosity.

One can think of mesoporosity as the onset of the QM to classical transition and visa-versa. Classical being the formation of the gas-liquid interface which is diffusely defined by the schichten equations in the QM, the schichten-gas-liquid interface (Sgl) transition.

*Example 2 The peak for mesoporosity SBA-15 silica:*

One should be able to calculate pore size with knowledge of the surface tension of the adsorptive and the value of  $\chi$  for the mesopore peak. The data by Guillet-Nicolas, Wainer, Marcoux, Thommes and Kleitz<sup>6</sup>(GWMTK) will be used for illustration. An isotherm was selected, which the adsorptive was N<sub>2</sub> at 78 K and the adsorbent is SBA-15 calcined at 413 K for 24 hours (S(140)24\_N.) The following constants were used:

$$\gamma_{lg,78K} = 8.72 \text{ mN m}^{-1}, \rho_{N_2(l)} = 0.809 \text{ g mL}^{-1} \Rightarrow \bar{V}_{N_2(l)} = 34.63 \text{ mL mol}^{-1}.$$

The nitrogen surface tension at 77K is from the UNIFAC (Dortmund) data base<sup>7</sup> with several authors in agreement. *Equation 4* was used for calculating the radius from energy.

This GWMTK sample was chosen because the graph was reasonably readable, and enough data points were present in critical areas. The isotherm and the pore size analysis are presented in **Error! Reference source not found.** and **Error! Reference source not found.**. A summary of the output data and derived quantities are presented in *Table 2*. In the NLDFT results by GWMTK is also presented for comparison. The spread in the NLDFT is much larger in the pore distribution than the QM results. However, the NLDFT assumes a hard core for the admolecules that should spread out the looks of the distribution, whereas the QM calculation is center-to-center.

In **Error! Reference source not found.** the calculation of the QM pore distribution used both the **D** distribution and the  $\chi^{-1}$  distribution. In **Error! Reference source not found.** the **N** companion distribution of the **D** function is the  $\times$ 's line. The solid line is the  $\chi^{-1}$  distribution. There is only a slight difference between the two.

In *Table 2* are the output parameters. The conversion to SI units uses the classical IUPAC conversions listed in the physical adsorption conventions<sup>8,9</sup>. For example, nitrogen has the classical molar area of  $9.77 \times 10^4 \text{ m}^2 \text{ mol}^{-1}$ , and the conversion from linear monolayer equivalence is IUPAC classical diameter of  $0.354 \text{ nm monolayer}^{-1}$ . Opposing sides, however, need to be counted. (The van der Waals  $d = 3.1 \text{ nm}$  and the following dimensions apply to solid N<sub>2</sub>: the waste is  $d_w = 0.339 \text{ nm}$ , and the length is  $d_l = 0.434 \text{ nm}$ . Thus classically, it makes a 20%

difference the orientation of N<sub>2</sub> to the surface.) The QM analysis does not predict that an outer liquid-gas boundary exists, at least in its present development. However, we know that it happens, and if it is a sudden enough formation, then there should be a peak in the observed  $\Delta H$  to indicate this. If the adsorbent is perfectly smooth, it may be that the transition is above a high  $\theta$  value ( $\geq 9$  monolayer equivalence<sup>\*</sup>), thus little heat is emitted and it is not noticed. So far, some smooth surfaces have absorbed up to 8 monolayer equivalences without any sudden shift, which contradict the prediction by Brunauer<sup>10, 11</sup>. Most likely, the sample becomes noticeably “wet.” This ends the experiment with adsorptive dripping off the side of the sample tube.

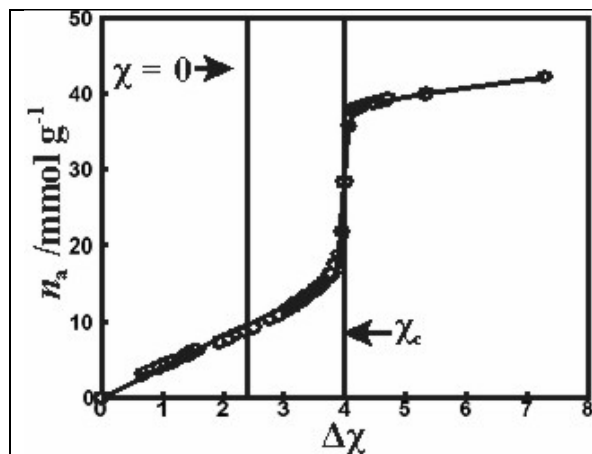


Figure 4 The isotherm fit to the data by GWMTK. sample S(140)24\_N. This is for the adsorption branch.

Used with permission of Science Direct-Elsevier Publishing

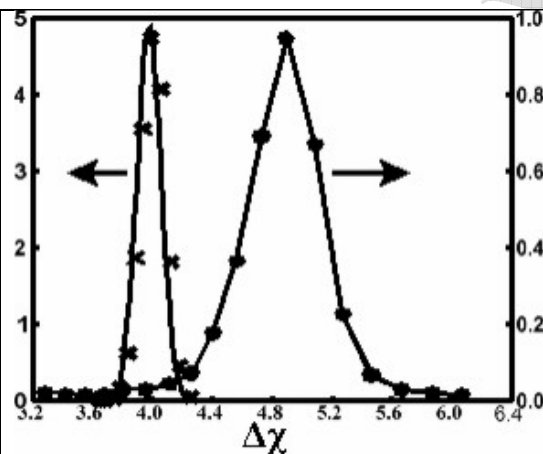


Figure 5 Pore size distribution,  $r$ , by:  
 ● the NLDFT by GWMTK  
 — line  $N$  distribution for NLDFT and  
 ✖ the distribution from the  $\chi^1$  function.

Some symbols assuming cylindrical pores used in this table include:

$d$  = pore diameter calculated wall to wall.

$r$  = the radius of the adsorbent pore wall to wall.

$t$  the classical “thickness” the QM is partial filling in monolayer equivalence

$t_m$  = classical monolayer “thickness” the QM monolayer equivalence

$p$  = “of the pore”

$\uparrow$  = “for adsorption”

$\downarrow$  = “for desorption”

\* Why would the transition not be seen at  $\Delta\chi = 8$ , assuming a high energy silica with a  $\chi_{cL} = -3.0$ , this means that measurement are made to  $\chi_{cL} = 5.0$  which is an energy of transition for N<sub>2</sub> of about  $-4.3 \text{ J mol}^{-3}$ . In comparison to the  $E_a = -13 \text{ kJ mol}^{-1}$  this is quite small.

Table 2 -Output parameters and quantities for data by GWMTK of N <sub>2</sub> on S(140)24_N sample					
Basic values and units from QM derivation.			derived from QM (*) or UPAC convention (‡)		
$n_m =$	3.979 <sup>(a)</sup>	mmol g <sup>-1</sup>	$A_{total} =$	388.7	m <sup>2</sup> g <sup>-1</sup> (*,‡)
$\langle \chi_s \rangle =$	-2.4163 <sup>(a)</sup>		$\langle \bar{E}_{a\uparrow} \rangle =$	-7.17	kJ mol <sup>-1</sup> (*)
$n_{ext} =$	1.071 <sup>(a)</sup>	mmol g <sup>-1</sup>	$A_{ext} =$	104.6	m <sup>2</sup> g <sup>-1</sup> (*,‡)
			$A_{p\uparrow} = A_{total} - A_{ext} =$	284.1	m <sup>2</sup> g <sup>-1</sup> (*,‡)
$n_{p\uparrow} =$	34.350 <sup>(a)</sup>	mmol g <sup>-1</sup>	$V_{p\uparrow} =$	$1.19 \times 10^{-6}$	m <sup>3</sup> g <sup>-1</sup> (*,‡)
			$d\uparrow = 4V_{p\uparrow}/A_{p\uparrow} =$	<b>16.8</b>	nm (*,‡)
			$t_m =$	0.709 <sup>(c)</sup>	nm (*)
$\langle \Delta\chi_{p\uparrow} \rangle =$	3.974 <sup>(a)</sup>	monolayers	$t = t_m \langle \Delta\chi_{p\uparrow} \rangle =$	2.82	nm (*,‡)
$\langle \chi_{p\uparrow} \rangle =$	1.5578	monolayers	$\langle \bar{E}_{p\uparrow} \rangle =$	-136.6	J mol <sup>-1</sup> (*)
			$r_{c(\langle \bar{E}_{p\uparrow} \rangle)} =$	2.21	nm (*,‡)
			$r\uparrow = r_c + t =$	5.03	nm (*,‡)
			$d_{p\uparrow} = 2r\uparrow =$	<b>10.06</b>	nm (*,‡)
			$A_{BET}^{(d)} =$	580	m <sup>2</sup> g <sup>-1</sup> (‡)
			$V^{(d)} =$	$1.42 \times 10^{-6}$	m <sup>3</sup> g <sup>-1</sup> (‡)
			$d\uparrow = 4V^{(d)}/A_{BET}^{(d)} =$	<b>9.79</b>	nm (‡)
			$d_{p\uparrow}^{(e)} =$	<b>10.1</b>	nm (‡)
$\sigma_p =$	$6.989 \times 10^{-2}$	monolayers	$\langle \bar{E}_{d\downarrow} \rangle =$	-270.8	J mol <sup>-1</sup> (*)
$\sigma_{fit} =$	0.6127	mmol g <sup>-1</sup>	$\langle \Delta\chi_{d\downarrow} \rangle =$	3.11	(*)
$\sigma\% \text{ FDR} =$	1.45 %		$m_{\downarrow}/m_{\uparrow} =$	1.98	(*)
(a) This indicates an output parameter.			FDR = “of Full Data Range”		
(b) Measured from admolecules’ centers					
(c) Measured across pore admolecules’ inside edges.					
(d) This datum is given by GWMTK					
(e) Given by GWMTK using NLDFIT <sup>12</sup> .					
$p_{\uparrow}$ = the pore value for adsorption $p_{\downarrow}$ = the pore value for desorption					
<b>Note: The values for the pore diameter are in bold font.</b>					

The first observation is that the  $\sigma\% \text{ FDR}$  is slightly out of the acceptable range but, certainly better than any other type of fit to this entire isotherm. It appears there are  $T$ -control problems at the beginning and there is uncertainty about  $\langle \chi_s \rangle$ . This will create uncertainty for the  $n_m$  and other vital parameters. However, this is for illustration of what to obtain from the isotherm, especially for the hysteresis. The data for the desorption was readable only in the hysteresis

region, but that is all that is needed for the energy of the mesopore transition. Thus, the pore peak energy could be read for both hysteresis branches. The value for the ratio  $m_{\downarrow}/m_{\uparrow}$  is almost ideal 2. This, however, may be fortuitous.

The calculations of the pore diameter from  $V$  and  $A$  does not yield the same value as the energy calculation. However, the assumption of ideal cylinders is not appropriate for a 3D intermeshed pore system. On the other hand, the pore calculation from energy is calculated for the core radius,  $r_c$ , and not for the adsorbent wall-to-wall radius. The classical film thickness,  $t$  at  $\langle \Delta\chi_p \rangle$  must be added to  $r_c$  to obtain  $r$ , the wall-to-wall adsorbent radius.

The  $A_{\text{BET}}$  is higher than the QM calculation, but the BET value for  $A$  is about twice the true value. That implies that it would have calculated 10 to 25 nm according to Part III. So, neither the corrected BET nor the QM can reliably calculate the pore radius by the ratio  $V/A$ . By coincidence the high value of the BET area brings it into a false agreement with the NLDFT results. This ratio obviously calculates another fractal quantity.

Another isotherm by GWMTK that has been analyzed is sample K(140)24\_N2. It is KIT-5 prepared with a 313 K treatment for 24 hrs, had a somewhat lower ratio of  $\sim 1.4$ , so the  $m_{\downarrow}/m_{\uparrow} = 2.0$  is probably not a common rule. The three examples though seem to indicate that  $1 \leq m_{\downarrow}/m_{\uparrow} \leq 2$ .

### Conclusion concerning mesoporosity:

So far, the QM/ESW hypothesis does an excellent job of fitting isotherms which include “simple case” and making modification for:

1. Heterogeneity
2. Microporosity and
3. Mesoporosity both adsorption and desorption and a potential start to explain
4. Hysteresis

The argument for the first three is very strong. For the fourth one, a lot more work is required. However, interpretation of the fitting parameters for mesoporosity is especially tentative for the phenomenon of hysteresis and converting to a model with IUPAC convention is more tentative. The question, “What is the precise definition of pore size and is this needed” is not clear. More high-quality experimentation and theoretical development is clearly needed to determine a practical definition and to what use this information be put to.

### What is next?

But what so far has been neglected herein? – An important question to guide future research:

More work relating the heats of adsorption to the isotherm data is needed with the technique and with equipment at least as good as that by Berg. Although there is some

data compiled in the literature<sup>13</sup>, there is only one publication that does a direct measurement with the same sample in the same combined equipment<sup>14,15,16</sup>. Much better controlled experiments are in order. As good as Berg's data is, there are still questions about the actual calculations made, knowing that the differential heat is, by nature, missing one critical data point.

The use of QM/ESW as applied to binary adsorptives looks like it might be possible. The use of the Langmuir isotherm has been tried, with only modest success<sup>17</sup> pre-magic point. The biggest problem in the endeavor has been the involved mathematics required, but of course, the Langmuir is not appropriate for the full isotherm or the very low pressures. It is however a relatively simple equation for use in differential equations. The  $\chi$ -transform would seem an easier route. Unfortunately, there does not seem to be enough basic research on even the simplest systems to start testing any derivation. Some suggestions and the use of two data sets is presented in the next part

These two topics, along with an overall summary and conclusion, is presented in Part VII.

### **Acknowledgements:**

I am thankful for the guidance received from Dr. E. Loren Fuller, Jr., who was a kind mentor to me and passed on the knowledge that started with Polanyi. I am grateful to W. Thomas Berg who provided me with his excellent thermodynamic data that provided a significant breakthrough. I also wish to thank Dr. Jürgen Adolphs for his encouragement, multiple discussions and confirmatory evidence for the theoretical developments.

### **Funding:**

This article was not funded.

### **Data and materials availability:**

All the data and materials are available in the open literature and are referenced herein.

### **References:**

---

<sup>1</sup> J. B. Condon, Using classical methods to start quantum mechanical calculations for microporosity and mesoporosity. *Adsorption* **26**, 1291–1299 (2020).

<sup>2</sup> R. Guillet-Nicolas, L. Marcoux, F Kleitz, *Insights into pore surface modification of mesoporous polymer-silica composites: introduction of reactive amines*, *New Journal of Chemistry*, , **34**, 355-366 (2010) **sup**: DOI: 10.1039/b9nj00478e

<sup>3</sup> J. B. Condon, *Surface Area and Porosity Determinations by Physisorption, Measurements, Classical Theories and Quantum Theory* (Elsevier, Amsterdam ed.2 fig. 6.19, 2020).

<sup>4</sup> D.Basmadjian, *The Little Adsorption Book – A practical Guide for Engineers and Scientists*, (CRC Press, 1997) ISBN: 0-8493-2692-3

<sup>5</sup> A. W. Adamson, *Physical Chemistry of Surface*, ed. 5. (John Wiley and Sons, Inc. 1990) p58 Eq. III-20 and p297 Eq VII-6.

<sup>6</sup> R. Guillet-Nicolas, M. Wainer, L. Marcoux, M. Thommes, F. Kleitz, J. Insights into pore surface modification of mesoporous polymer-silica composites: Introduction of reactive amines. *Colloid Interface Sci.* **579**, 489–507 (2020)

<sup>7</sup>UNIFAC, “Modified UNIFAC (Dortmund) and the Predictive Equations of State PSRK and VTP” [http://unifac.ddbst.de/en/EED/PCP/SFT\\_C1056.php](http://unifac.ddbst.de/en/EED/PCP/SFT_C1056.php) - also see: (Dortmund Data Base, DDB #1057, Nitrogen, CAS = 7727-37-9.)

<sup>8</sup> M. Thommes, K. Kaneko, A. V. Neimark, J. P. Olivier, F. Rodriguez-Reinoso, J. Rouquerol, K. S. W. Sing, Physisorption of gases, with special reference to the evaluation of surface area and pore size distribution (IUPAC Technical Report), *Pure Appl. Chem.*, **87(9-10)** 1051–1069 (2015).

<sup>9</sup> K. S. W. Sing, D. H. Everett, R.A.W. Haul, L. Moscou, R. A. Pierotti, J. Rouquerol, T. Siemieniewska, International Union of Pure and Applied Chemistry, Physical Chemistry, commission on Colloid and Surface Chemistry Including Catalysis, Reporting Physisorption Data for Gas/Solid Systems with Special Reference to the Determination of Surface Area and Porosity. *Pure & Appl. Chem.* **57(3)**, 603-619 (1985).

<sup>10</sup> S. Brunauer, *The Adsorption of Gases and Vapor - Volume 1 Physical Adsorption* (Princeton University Press, 1942),(Oxford University Press, 1946) p194 in the Legare Street Press release.

<sup>11</sup> W. E. Fuller Jr.,– Private discussion with S. Brunauer requested by JBC.

<sup>12</sup> P.I. Ravikovitch, A.V. Neimark, Characterization of Micro- and Mesoporosity in SBA-15 Materials from Adsorption Data by the NLDFT Method. *J. Phys. Chem. B*, **105** 6817–6823 (2001).

<sup>13</sup> J.B. Condon, Heats of physisorption and the predictions of chi theory. *Microporous Mesoporous Mat.* **33**, 21-36 (2002).

<sup>14</sup> W. T. Berg, “Heat Capacities from 15-140 K and Entropies of Krypton Adsorbed On Anatase,” PhD Thesis, Western Reserve University (now Case Western Reserve University) Cleveland, OH, USA (1955)

<sup>15</sup> E. L. Pace, K. S. Dennis, W, T, Berg, **Error! Main Document Only.** Thermodynamic properties of krypton adsorbed on titanium dioxide (rutile). *J. Chem. Phys.* **23**, 2166-2168 (1955).

<sup>16</sup> E. L. Pace, W, T, Berg, A. R. Siebert, Entropy of Krypton Adsorbed on Titanium Dioxide (Anatase). *J. Am. Chem. Soc.* **78(8)**, (1956) 1531-1533.